

1 Modern and Reproducible Groundwater Modeling Workflows with
2 FloPy

3 Joseph D. Hughes¹, Christian D. Langevin², Scott R. Paulinski³, Joshua D. Larsen⁴, and
4 David Brakenhoff⁵

5 ¹U.S. Geological Survey, Model Support and Maintenance Branch, 927 W Belle Plaine Ave,
6 Chicago, IL, USA

7 ²U.S. Geological Survey, Model Support and Maintenance Branch, 2280 Woodale Dr, Mounds
8 View, MN, USA

9 ³U.S. Geological Survey, California Water Science Center, 4165 Spruance Road, Suite 200, San
10 Diego, CA, USA

11 ⁴U.S. Geological Survey, California Water Science Center, 6000 J Street, Placer Hall,
12 Sacramento, CA, USA

13 ⁵Artesia Water, Korte Weistraat 12, Schoonhoven, Netherlands

14 November 16, 2022

15 **Abstract**

16 FloPy functionality has been expanded from the capabilities described in Bakker et al. (2016) to
17 support the latest version of MODFLOW (MODFLOW 6). FloPy classes are automatically generated
18 using the same files used to generate the MODFLOW 6 input guide, which allows new features
19 to be supported immediately and FloPy to be a critical component for MODFLOW 6 development
20 and testing. FloPy can be used to download MODFLOW-based and other executables for Linux,
21 MacOS, and Windows operating systems, which simplifies the process required to download and use
22 these executables. Expanded FloPy capabilities include (1) full support for structured (DIS), layer-
23 based unstructured (DISV), and fully-unstructured (DISU) MODFLOW 6 discretization types; (2)
24 geoprocessing of shapefile-like and raster data to develop model data for all MODFLOW 6 discretization
25 types; (3) the addition of functionality to provide user-centric access to simulated output data;
26 (4) extension of plotting capabilities to unstructured MODFLOW 6 discretization types; and (5)
27 the ability to export model, package, and individual array data to shapefiles, NetCDF, and VTK
28 formats for processing, analysis, and visualization by other software products. Examples of using
29 expanded FloPy capabilities are presented for a hypothetical watershed. An unstructured ground-
30 water flow and transport model, with several advanced stress packages, is presented to demonstrate
31 how FloPy can be used to develop complicated model datasets from original source data (shapefiles
32 and rasters), post-process model results, and plot simulated results.

33 **1 Introduction**

34 FloPy is a [popular](#) Python package for constructing, running, and post processing MODFLOW-based
35 groundwater flow and transport models (Bakker et al. 2016). It is [an open-source Python package](#)
36 developed by a growing community of contributors. The combination of open-source programming
37 languages (such as Python) with version control software (such as Git) allow the model construction
38 process to be documented, reproducible and easily inspected and used by others. This workflow has

39 been recommended as one way to facilitate repeatable research and sharing of ideas (Fienen and Bakker
40 2016). Bakker et al. (2016) describe the general approach for working with models within the Python
41 environment and emphasize the reproducible nature of developing models through scripting.

42 FloPy has been used to pioneer new methods and analysis tools, such as deep learning approaches
43 for improving groundwater model calibration (Sun 2018; Zhou and Tartakovsky 2021), regionalizing
44 residence times using metamodeling (Starn and Belitz 2018), applying iterative ensemble approaches
45 for calibration and uncertainty quantification (White 2018), and exploring alternative parameteriza-
46 tion schemes for risk analysis (Knowling et al. 2019). There are numerous examples of constructing
47 MODFLOW models with FloPy to solve applied groundwater problems (Befus et al. 2017; van Engelen
48 et al. 2018; Ebeling et al. 2019; Zipper et al. 2019; Befus et al. 2020). FloPy is used in GIS-based tools,
49 such as FREEWAT (Rossetto et al. 2018) and other cyberinfrastructures (Essawy et al. 2018) to export
50 models into MODFLOW datasets. FloPy can also be used as the “glue” to help couple MODFLOW
51 to other hydrological models (Burek et al. 2020) or, for example, to agent-based models designed to
52 quantify the effects of decision makers on environmental behavior (Jaxa-Rozen et al. 2019).

53 We use FloPy extensively to teach MODFLOW and groundwater modeling to early- and mid-career
54 engineers and scientists. Other organizations also use FloPy to teach MODFLOW (for example, Hatari
55 Labs and the Australian Water School). Annotated Jupyter notebooks and example scripts ~~are useful~~
56 ~~for demonstrating~~ concepts and provide a resource that can be used as templates for developing real-
57 world model applications. We routinely rely on FloPy to load and help identify problems in user model
58 applications, and with the initial release of the MODFLOW 6 groundwater flow model (Langevin et al.
59 2017), we started to rely on FloPy to help with development of the MODFLOW program. We write
60 tests that rely on FloPy to construct and run models, and then read output. We then verify that the
61 output is as expected, by using analytical solutions, other models, or results that have been confirmed
62 to be correct.

63 The purpose of this paper is to highlight important FloPy advances since it was first described
64 by Bakker et al. (2016), provide examples that demonstrate these new capabilities, and reinforce
65 the advantages of the modern scripting workflow for developing reproducible groundwater flow and
66 transport models that can be easily updated as new data become available. The important advances
67 described here include (1) complete support for all models, packages, and options implemented in the
68 core version of MODFLOW supported by the U.S. Geological Survey (Hughes et al. 2017; Langevin
69 et al. 2017; Provost et al. 2017; Langevin et al. 2020; Morway et al. 2021; Langevin et al. 2022; Hughes
70 et al. 2022; Mancewicz et al. 2022); (2) generalized support for models based on a regular grid consisting
71 of layers, rows, and columns, and also for models based on unstructured grids; (3) implementation of
72 new geoprocessing capabilities to rapidly populate models with data from a variety of input sources;
73 (4) simplified access to model results; (5) plotting capabilities for map and cross-section views of model
74 data; and (6) export capabilities for writing model data to a variety of output formats.

75 2 FloPy Support for MODFLOW 6

76 The most recent version of MODFLOW (MODFLOW 6) is an object-oriented program and framework
77 developed to provide a platform for supporting multiple models and multiple types of models within
78 the same simulation (Hughes et al. 2017). These models can be independent of one another with no
79 interaction, they can exchange coefficients and dependent variables (for example, head), or they can
80 be tightly coupled at the matrix level by adding them to the same numerical solution. Transfer of
81 information between models is isolated to exchange objects, which allow models to be developed and
82 used independently. Within this new framework, a regional-scale groundwater model may be coupled
83 with multiple local-scale groundwater models.

84 MODFLOW 6 currently includes the Groundwater Flow (GWF) Model and the Groundwater

85 Transport (GWT) Model each with packages to represent surface water processes, groundwater ex-
86 traction, external boundaries, mass sources and sinks, and mass sorption and reactions. GWF and
87 GWT models can be developed using regular model grids consisting of layers, rows, and columns or
88 they can be developed using more general unstructured grids using many of the concepts and numerical
89 approaches available in MODFLOW-USG ([Panday et al. 2013](#)). MODFLOW 6 also includes advanced
90 formulations to simulate three-dimensional anisotropy and dispersion ([Provost et al. 2017](#)), coupled
91 variable-density groundwater flow and transport ([Langevin et al. 2020](#)), and a water mover package to
92 represent natural and managed hydrologic connections ([Morway et al. 2021](#)).

93 Development and testing of the MODFLOW 6 program relies heavily on tight integration with
94 FloPy. A key component of this tight integration is the capability to quickly support new MODFLOW
95 6 models and packages with FloPy. Unlike the FloPy support for previous MODFLOW versions (for
96 example, MODFLOW-2005, MODFLOW-NWT, MODFLOW-USG, and SEAWAT), the FloPy Python
97 classes for MODFLOW 6 are dynamically generated from simple text files, called “definition files,” that
98 describe the input file structure (Figure 1). All MODFLOW 6 model input files are described using
99 these definition files. This allows MODFLOW 6 developers to write tests for new models, packages,
100 and functionality as they are developed. These definition files are used to generate the user input
101 and output guide. These same definition files are also used to generate FloPy classes, with argument
102 docstrings corresponding to input variable descriptions in the input and output guide. ~~Definition~~
103 ~~files used to create FloPy Python classes for MODFLOW 6 are located in the flopy/mf6/data/dfn/~~
104 ~~subdirectory in the site-packages directory for a Python distribution or Python environment.~~ The
105 FloPy Python classes for MODFLOW 6 can be regenerated using

```
106     >>> import flopy  
107     >>> flopy.mf6.utils.createpackages.create_packages()
```

108 New functionality can be added by users to existing packages by modifying existing definition files
109 using instructions provided in the [MODFLOW 6 GitHub repository](#). The existing definition files
110 can also be used as a template for creating classes for new MODFLOW 6 models or packages.
111 New definition files should be placed in the `flopy/mf6/data/dfn/` subdirectory prior to rerunning
112 `flopy.mf6.utils.createpackages.create_packages()`.

113 3 Common Modeling Tasks

114 3.1 Getting MODFLOW and Other Related Executables

115 FloPy for MODFLOW 6 relies on a number of helper classes, which wrap functionality available in
116 pre-compiled external executables, to generate unstructured models and calculate water budgets on
117 user-defined zones. To facilitate getting these executables and other MODFLOW and related programs
118 (for example, MODPATH, MT3DMS, MT3D-USGS, SEAWAT, etc.) can be installed using

```
119     get-modflow :flopy
```

120 in a terminal or at the command line after installing FloPy. The `get-modflow` command downloads
121 the latest release of MODFLOW and related programs for the operating system the command is run
122 on (Windows, MacOS, or Linux) from an [Executables GitHub repository](#). `get-modflow` can also
123 download previous versions of MODFLOW 6 and the latest development version of MODFLOW 6
124 using instructions available on the [FloPy GitHub repository](#).

MODFLOW 6 Input and Output Guide

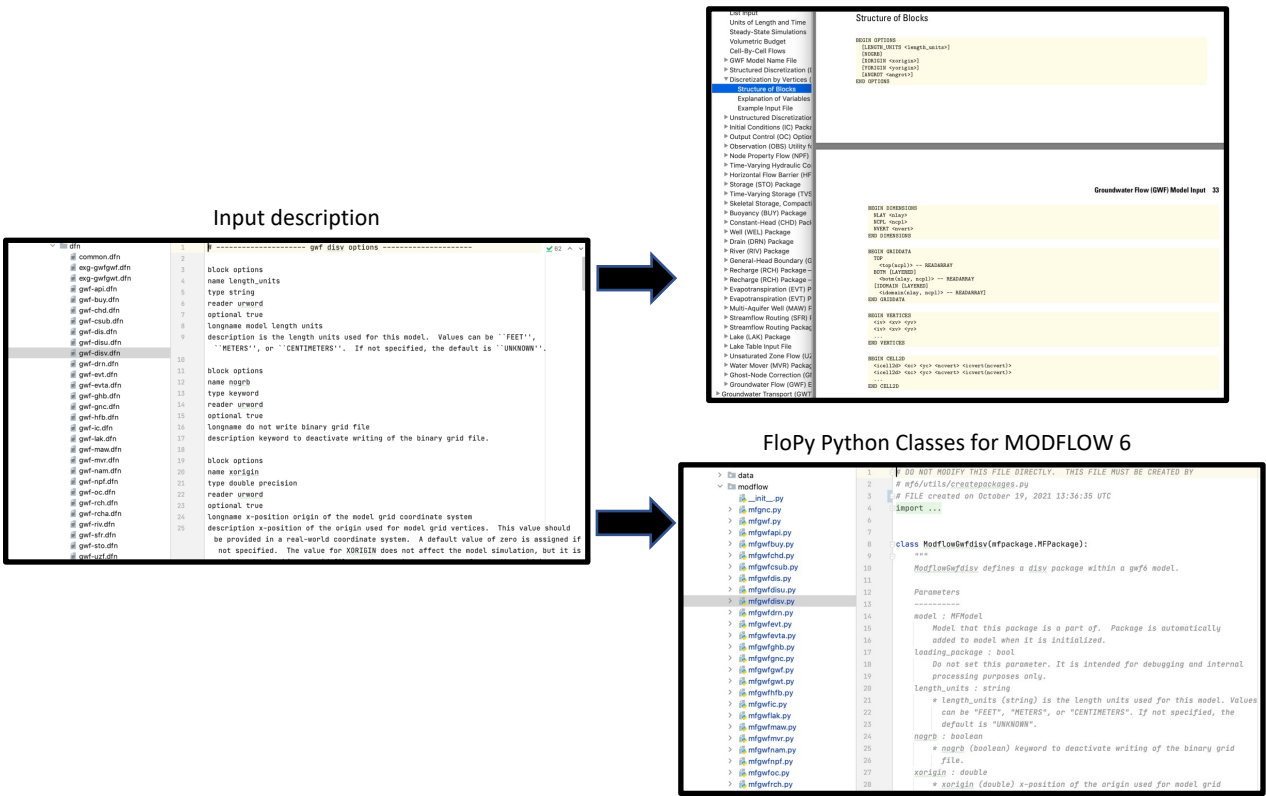


Figure 1: Relation between MODFLOW 6 input description files and the MODFLOW 6 input and output guide and the FloPy Python classes for MODFLOW 6.

125 3.2 Managing and Creating Model Grids

126 FloPy was originally developed to support models that are based on a regular grid consisting of lay-
 127 ers, rows, and columns. With recent support for unstructured grids in MODFLOW (Panday et al.
 128 2013; Langevin et al. 2017) it became necessary to revise the underlying approach for managing spa-
 129 tial discretization information in FloPy. The goal was to containerize grid information into a single
 130 location and use this information throughout FloPy modeling tasks for geospatial processing, plot-
 131 ting, and exporting. Spatial discretization is now handled in FloPy through dedicated model grid
 132 classes. There is a **Grid** class, which serves as the base class for the **StructuredGrid**, **VertexGrid**,
 133 and **UnstructuredGrid** classes. Grid objects can be created by the user for preprocessing, and they
 134 will be automatically generated and attached to a FloPy model object.

135 Regular MODFLOW grids can have constant row and column spacings, as shown in Figure 2A, or
 136 they can have variable row and column spacings to focus resolution around an area of interest, as shown
 137 in Figure 2B. The following Python code shows how to create a **StructuredGrid** object in FloPy. A
 138 **StructuredGrid** object will also be created from discretization data required when instantiating a
 139 MODFLOW 6 DIS object using `flopyp.mf6.ModflowGwfdis()`.

```
140 >>> regular_grid = flopyp.discretization.StructuredGrid(nlay=nlay,
141 ... delr=delr, delc=delc, xoff=0.0, yoff=0.0, angrot=0.0, top=top, botm=botm)
```

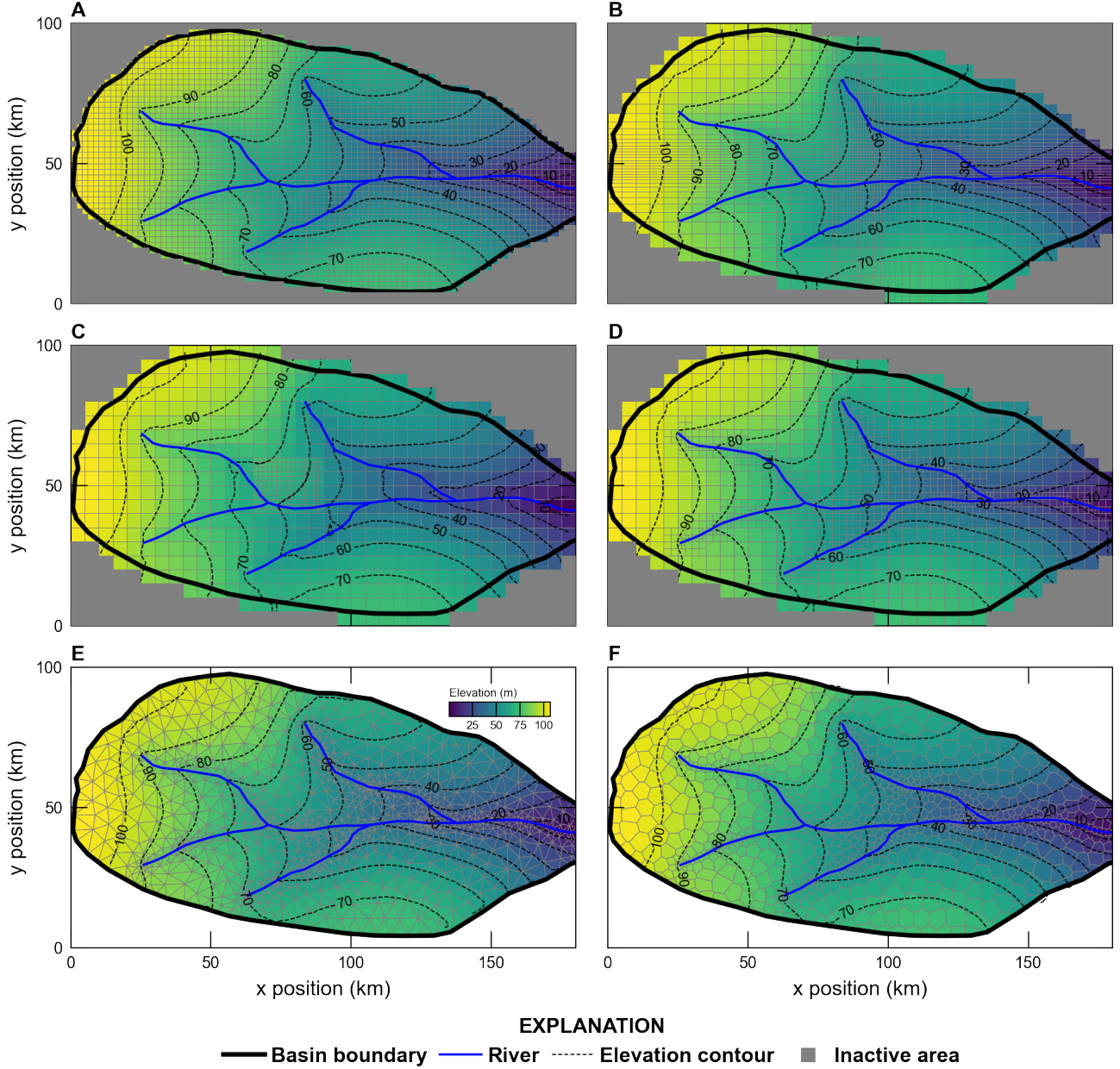


Figure 2: Examples of grids that can be generated and processed using FloPy for a hypothetical watershed, including (A) a regular MODFLOW grid with constant and equal row and column spacings, (B) a regular MODFLOW grid with variable row and column spacings, (C) a regular MODFLOW child grid nested within a regular MODFLOW parent grid, (D) a quadtree grid generated with the GRIDGEN program (Lien et al. 2014) through the FloPy wrapper, (E) a triangular grid generated with the Triangle program (Shewchuk 1996) through the FloPy wrapper, and (F) a Voronoi grid created from the triangular mesh.

142 MODFLOW 6 was developed to natively support multi-model simulations (Hughes et al. 2017).
 143 One form of multi-model simulation is a nested grid application in which a more finely discretized child
 144 model is embedded within a more coarsely discretized parent model (Mehl and Hill 2006; Vilhelmsen
 145 et al. 2012; Mehl and Hill 2013). The use of a locally refined grid (LGR) within a parent grid offers

146 computation benefits in that the additional refinement is targeted to an area of interest. FloPy provides
147 a utility class, called `Lgr()` for constructing the data required to tightly couple parent and child models
148 within a single MODFLOW 6 simulation. Figure 2C shows two `StructuredGrid` objects—one object
149 represents the parent model grid and the other represents the nested child grid. The `Lgr()` class defines
150 the connection properties between cells in the parent model and cells in the child model. The utility
151 is general in that the child model can have more layers than the parent model.

152 FloPy supports management and generation of unstructured grids. Unstructured grids are rep-
153 resented in FloPy as being layered or fully unstructured. A layered grid is one in which the same
154 grid applies to all model layers. An unstructured grid is more general and allows the model grid to
155 change with depth. Layered grids and unstructured grids are stored in FloPy as `VertexGrid` and
156 `UnstructuredGrid` objects, respectively.

157 A layered quadtree grid can be created with FloPy using the `Gridgen()` utility class, which is a
158 wrapper around the GRIDGEN program (Lien et al. 2014). GRIDGEN starts with a regular MOD-
159 FLOW grid provided by the user. The program then recursively subdivides individual cells that
160 intersect with refinement features into quarters until a maximum level of refinement is met. Refine-
161 ment features may be points, lines, or polygons. Smoothing is automatically handled so that a cell is
162 connected to no more than two cells in any primary horizontal direction and four cells in the vertical
163 direction. Figure 2D shows an example of a quadtree grid created with GRIDGEN in which a base
164 grid is refined along streams. The following Python code shows the steps for creating the quadtree
165 grid with GRIDGEN.

```
166 >>> sim = flopy.mf6.MFSimulation()  
167 >>> gwf = flopy.mf6.ModflowGwf(sim)  
168 >>> dis6 = flopy.mf6.ModflowGwfdis(gwf, nrow=nrow, ncol=ncol, delr=dy, delc=dx)  
169 >>> g = Gridgen(dis6, model_ws=temp_path)  
170 >>> g.add_refinement_features([[closed_polygon]], "polygon", 0, range(1))  
171 >>> g.add_refinement_features(stream_points, "line", 2, range(1))  
172 >>> g.build(verbose=False)  
173 >>> gridprops_vg = g.get_gridprops_vertexgrid()  
174 >>> quadtree_grid = flopy.discretization.VertexGrid(**gridprops_vg)
```

175 FloPy also provides a wrapper utility for the Triangle mesh generation program (Shewchuk 1996).
176 The `FloPy.Triangle()` utility class writes the Triangle program input file, runs the Triangle program,
177 and then loads the triangular mesh. Users provide the maximum area for individual triangles, angle
178 constraints, a polygon describing the model domain, and so forth. Figure 2E shows an example of a
179 triangular grid created with the Triangle program. The Python code for creating the triangular grid
180 is shown below.

```
181 >>> tri = flopy.utils.triangle.Triangle(maximum_area=maximum_area,  
182 ... angle=30, nodes=nodes, model_ws=temp_path)  
183 ...  
184 >>> tri.add_polygon(boundary_points)  
185 >>> tri.build(verbose=False)  
186 >>> cell2d = tri.get_cell2d()  
187 >>> vertices = tri.get_vertices()  
188 >>> triangular_grid = VertexGrid(vertices=vertices, cell2d=cell2d,  
189 ... idomain=idomain, nlay=nlay, ncpl=tri.ncpl, top=top, botm=botm)
```

191 A triangular grid can be converted into a Voronoi grid using the `VoronoiGrid()` utility class within
 192 FloPy. This utility class uses SciPy routines (Virtanen et al. 2020) to construct Voronoi polygons
 193 around each vertex in the triangular mesh. Figure 2F shows an example of a Voronoi grid created from
 194 the triangular mesh shown in Figure 2D. The steps for creating the Voronoi grid from the `Triangle`
 195 object are shown below.

```
196 >>> vor = flopy.utils.voronoi.VoronoiGrid(tri)
197 >>> gridprops = vor.get_gridprops_vertexgrid()
198 >>> voronoi_grid = VertexGrid(**gridprops, nlay=nlay, idomain=idomain)
```

199 `StructuredGrid`, `VertexGrid`, and `UnstructuredGrid` grid objects have useful properties (`_property`)
 200 and methods (`_method()`) for accessing or mapping locations on the model grid including: (1) con-
 201 version of xy pairs from local to global coordinates (`.get_coords()`) and from global to local coor-
 202 dinates (`.get_local_coords()`); (2) getting x, y, and z coordinates for cell centers (`.xcellcenters`,
 203 `.ycellcenters`, `.zcellcenters`, and `.xyzcellcenters`) and vertices (`.xvertices`, `.yvertices`, `.zvertices`,
 204 and `.xyzvertices`); (3) intersecting a list of xy pairs with the grid and returning the appropriate
 205 cellid (`.intersect()`). Other interesting grid object properties and methods include generating a
 206 grid object from a MODFLOW 6 binary grid file (`.from_binary_grid_file()`), calculating the cell
 207 thickness for each cell (`.thick`), and the saturated thickness for each cell (`.saturated_thick`).

208 The ability to develop model grid types using FloPy allows for innovation in the way a study area
 209 is discretized in order to tailor the grid to the needs of the study. For example, Guira (2018) used a
 210 Voronoi grid to add additional resolution in the vicinity of irrigation wells in the Frenchman Creek Basin
 211 in Nebraska, USA to quantify the effects of land-use change and irrigation on streamflow depletion.
 212 Furthermore, the ability to develop multi-model simulations using FloPy allows higher-resolution inset
 213 models to be added in focused areas. Fienen et al. (2022) used focused inset models implicitly coupled
 214 to a coarse regional model and solved as a single system of equations to better represent lakes and
 215 quantify lake/groundwater interactions in the Central Sands region in Wisconsin, USA. Inset models
 216 of lakes in Fienen et al. (2022) were developed using `modflow-setup` (Leaf and Fienen 2022), which
 217 relies on FloPy functionality to generate MODFLOW 6 datasets.

218 3.3 Geospatial Processing

219 Geospatial processing is often a fundamental part of creating a groundwater model. New geospatial
 220 processing functionality has been added to FloPy to help users construct models using data from
 221 common input sources. The geospatial processing functionality has been implemented to work with
 222 the different types of model grids so that it is straightforward to build and construct models with
 223 different grid resolutions or grid types. The geospatial processing routines work with all three of the
 224 model grid types (`StructuredGrid`, `VertexGrid`, and `UnstructuredGrid`).

225 A common geospatial processing task is resampling of raster data onto a model grid. For example,
 226 it is often necessary as part of model construction to resample a raster data set of land surface elevation
 227 onto a model grid. FloPy includes a new raster sampling utility based on the Rasterio Python package
 228 (Gillies et al. 2013). The following Python code demonstrates the steps for resampling an Esri ASCII
 229 raster format grid onto a Voronoi grid.

```
230 >>> fine_topo = flopy.utils.Raster.load("./grid_data/fine_topo.asc")
```

```

231     >>> top_vg = fine_topo.resample_to_grid(voronoi_grid, band=fine_topo.bands[0],
232         ... method="linear", extrapolate_edges=True)
233     ...

```

234 The result of raster resampling is a numpy array, equal in size to the number of cells in the Voronoi
 235 grid, with an interpolated land surface elevation for each model cell. In this Python code example, the
 236 land surface grid was interpolated to the Voronoi grid using a “linear” method, however, the method
 237 also supports other options (nearest, cubic, mean, median, min, and max) for resampling. The color
 238 floods of elevation in Figure 2 show the results of linear raster resampling for land surface onto a variety
 239 of structured and unstructured model grids.

240 Performing intersections of hydrologic features with the model grid is another common modeling
 241 task. FloPy is now equipped with robust and efficient capabilities for intersecting a model grid with
 242 points, lines, and polygons. The underlying intersection routines rely on the Shapely Python package
 243 (Gillies 2022) to determine intersection properties. When a point or collection of points is intersected
 244 with a model grid, the grid intersection routine returns the cells that intersect with the points. When
 245 a line or collection of lines is intersected with a model grid, the grid intersection routine returns the
 246 cells that intersect with the lines and the lengths of lines within the cell. The line and grid intersection
 247 routine also creates and returns individual line segments of the line features within each intersected cell.
 248 When a polygon or collection of polygons is intersected with a model grid, the grid intersection routine
 249 returns the cells that intersect with the polygons and the polygon area within the cell. The polygon and
 250 grid intersection routine also creates and returns individual polygons of the original polygon features
 251 within the intersected cells.

252 The following Python code demonstrates the steps for identifying the grid cells that intersect with
 253 a collection of line segments.

```

254     >>> ixs = flopy.utils.GridIntersect(voronoi_grid, method="vertex")
255     >>> cellids = []
256     >>> for points in segments:
257         ...     segment = ixs.intersect(LineString(points), sort_by_cellid=True)
258         ...     cellids += segment["cellids"].tolist()
259     ...

```

260 The result of this code snippet is a list of Voronoi grid cell numbers (called “cellids”) that intersect
 261 with the model grid. The `ixs.intersect()` method also returns the “lengths” of the shapelike
 262 collection intersecting each cell, the “vertices” corresponding to each cell that intersects a collection
 263 of shapelike objects, and a shapely object (“ixshape”) each portion of the original shapelike collection
 264 that intersects a cell. Results of the grid intersection for a linear stream network and the six different
 265 model grids is shown in Figure 3.

266 3.4 Processing MODFLOW 6 output

267 MODFLOW 6 has many different types of output that can be created during a simulation. A GWF
 268 Model, for example, can write simulated heads and detailed budget information to binary files. Global
 269 model budgets can be written to comma-separated value text files. Some individual GWF and GWT
 270 Model advanced stress packages can also write simulated output during a simulation. For example,
 271 the Lake (LAK) Package can write simulated lake stages and detailed lake budget information to
 272 binary files. Likewise, the Multi-Aquifer Well (MAW) Package can write simulated well head and well
 273 budgets to binary files. Recent improvements have been made to FloPy to allows users easier access

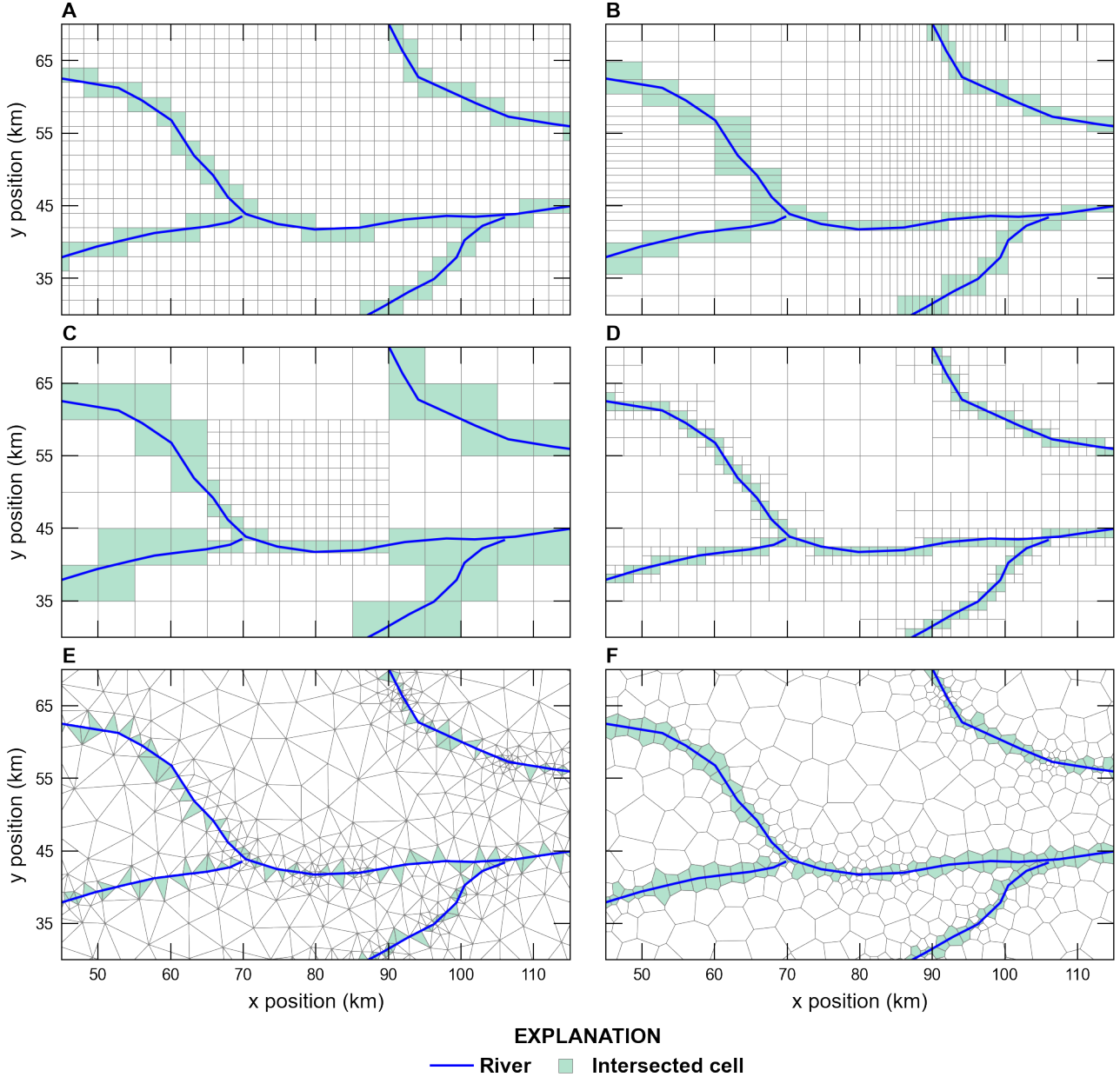


Figure 3: Examples of the intersection of a linear stream network with the model grids shown in Figure 2. Intersections were performed using FloPy for (A) a regular MODFLOW grid, (B) a regular MODFLOW grid with variable row and column spacing, (C) a regular MODFLOW child grid nested within a regular MODFLOW parent grid, (D) a quadtree grid, (E) a triangular grid, and (F) a Voronoi grid. Shaded cells represent those cells that intersect with the linear stream network. Individual plots in this figure are centered on the location of the child grid shown in Figure 2C.

274 to simulation results using `.output` routines. Prior to these improvements, users were required to
 275 instantiate head, concentration, and budget file readers using file paths and names in order to access
 276 this information. With the `.output` routines, the readers are automatically generated when called by
 277 the user.

278 The following `.methods()` syntax shows how a user can discover the type of output information
279 that is available for the specified `gwf` model.

```
280     >>> gwf.output.methods()  
281     ['list()', 'zonebudget()', 'budget()', 'budgetcsv()', 'head()']
```

282 The `.list()` method can be used to get the incremental (`incremental=True`) or cumulative budget
283 information for the `gwf` model for a user-specified simulation time, zero-based time step–stress period
284 tuple, or zero-based index. The `.zonebudget` method allows the user to easily build a Zone Budget for
285 MODFLOW 6 instance, then run the Zone Budget program, and view output. The `.budget()` method
286 gives user access to data in binary MODFLOW 6 cell-by-cell budget files. The `.budgetcsv()` method
287 gives user access to cumulative and incremental global budget data saved to a comma separated values
288 file. The `.head()` method gives user access to data in the binary MODFLOW 6 head file.

289 Similarly, The following `.methods()` syntax shows how a user can discover the type of output
290 information that is available for advanced stress packages like the LAK package.

```
291     >>> gwf.lak.output.methods()  
292     ['zonebudget()', 'budget()', 'budgetcsv()', 'package_convergence()', 'obs()',  
293     'stage()']
```

294 The `.package_convergence()` method can be used to get the convergence information for an advanced
295 stress package. The `.obs()` method can be used to get observation data saved for a model or stress
296 package as a numpy record array or pandas data frame. The `.stage()` method is the dependent
297 variable for the LAK package and is equivalent to the `.head()` method for the `gwf` model.

298 3.4.1 Processing simulated dependent-variable data

299 Dependent-variable data (for example, head or concentration) for a MODFLOW 6 groundwater flow
300 or transport model can be accessed using the `.output()` method on the GWF or GWT model, re-
301 spectively. To access the simulated head output, for example, a call can be made to the head reader
302 to retrieve data for a specified simulation time using the `.get_data()` method as follows.

```
303     >>> head = gwf.output.head().get_data(totim=1.0)
```

304 In this case, the `head` variable is a numpy array equal in size to the size of the model grid. Head data
305 can also be accessed for a zero-based time step–stress period tuple

```
306     >>> head = gwf.output.head().get_data(kstpkper=(0,0))
```

307 or a zero-based index

```
308     >>> head = gwf.output.head().get_data(idx=0)
```

309 in addition providing a user-specified simulation time (`totim=`).

310 **3.4.2 Processing simulated cell-by-cell budget results**

311 Similar to head output, cell-by-cell budget information can be accessed using FloPy. Unlike the
312 simulated head file, the cell-by-cell budget file can have data for more than one item, which can be
313 either arrays or lists of data. The data in the cell-by-cell budget file can be determined using

```
314 >>> gwf.output.budget().list_unique_records()
315      RECORD          IMETH
316      -----
317      FLOW-JA-FACE    1
318      DATA-SPDIS     6
319      DATA-SAT       6
320      WEL            6
321      DRN            6
322      RCHA           6
323      EVTA           6
324      SFR            6
325      LAK            6
```

326 The IMETH code indicates if the data is an array (IMETH=1) or is list based (IMETH=6). Cell-by-cell
327 specific-discharge data can be extracted using

```
328 >>> spdis = gwf.output.budget().get_data(totim=1.0, text="DATA-SPDIS")[0]
```

329 Specific-discharge data is returned as a list containing a Numpy record array for the user-specified
330 simulation time (totim=). Like MODFLOW head data, all of the data in the cell-by-cell data file for
331 a user-specified simulation time (totim=), zero-based time step-stress period tuple (kstpkper=), or
332 zero-based index (idx=) can also be extracted. Specific-discharge data can be processed into a form
333 that can be plotted with FloPy using

```
334 >>> qx, qy, qz = flopy.utils.postprocessing.get_specific_discharge(spdis, gwf,
335 ... head=head)
```

336 The optional argument head= above sets the specific-discharge in inactive or dry cells to NaN. ~~The~~
337 ~~get_specific_discharge()~~ method also includes functionality to plot specific discharge values at the
338 cell "centers" (default), "faces" or "vertices".



339 **3.4.3 Performing zone budgets analyses**

340 `zonebudget()` output methods are available for both the `gwf` model and the `gwf.lak` advanced stress
341 package examples shown above since they both solve a continuity equation. ~~The other~~ flow and
342 transport advanced stress packages also solve continuity equations and can be used with this Zone
343 Budget functionality. The `zonebudget()` output method can be used to perform a Zone Budget
344 analysis on the LAK advanced stress package using

```
345 >>> zonbud = gwf.lak.output.zonebudget(zarr)
```

```

346     >>> zonbud.write_input()
347     >>> zonbud.run_model()
348     FloPy is using the following executable to run the model: zbud6
349             ZONEBUDGET Version 6
350             U.S. GEOLOGICAL SURVEY
351             VERSION 6.3.0 03/04/2022
352
353 Normal Termination
354 (True, [])

```

355 zarr in the `gwf.lak.output.zonebudget()` is a numpy array that defines an integer zone for each
 356 lake in the LAK advanced stress package. Zone Budget output can be returned as a numpy record
 357 array (`.get_budget()` or `get_volumetric_budget()`) or a panda dataframe (`get_dataframes()`).

358 3.5 Plotting

359 FloPy plotting functions presented in Bakker et al. (2016) have been updated to support plotting
 360 both structured and unstructured models in map and cross-section view using the `.PlotMapView()`
 361 and `.PlotCrossSection()` classes, respectively. The plotting methods are thin wrappers around the
 362 matplotlib plotting methods (Hunter 2007) and allow fine-grained control using matplotlib keyword
 363 arguments (`kwargs`). The following Python code demonstrates the steps for plotting a map of simulated
 364 heads, the model grid, the location of drain (DRN) package cells, specific-discharge vectors, and head
 365 contours for the `gwf` model.

```

366     >>> mm = flopy.plot.PlotMapView(model=gwf)
367     >>> mm.plot_array(head, edgecolor="0.5")
368     >>> mm.plot_bc("DRN")
369     >>> mm.plot_grid()
370     >>> cs = mm.contour_array(head)
371     >>> mm.ax.clabel(cs)
372     >>> mm.plot_vector(qx, qy, normalize=True)
373     >>> plt.show()

```

374 Figure 4A shows the outcome of the Python code demonstrated above with additional geographic
 375 features and fine-grained control of grid lines, text, annotations, tick locations, and axis labels. Results
 376 shown in Figure 4 are for a steady-state model discretized into three convertible layers, with isotropic
 377 hydraulic properties, a hydraulic conductivity of 1 m/d, with rivers represented a drain cells, with
 378 drains located on the top of the model in layer 1 to prevent groundwater levels from exceeding the
 379 top of the model, and with an areal recharge rate of 0.000001 m/d. Figure 4B shows use of the
 380 `.plot_array()` method to create a map of the layer containing the water table, drain cells where the
 381 groundwater is discharging to a river, and cells where groundwater is discharging to the surface.

382 The following Python code demonstrates the steps for plotting a cross-section of simulated heads
 383 and the model grid for the `gwf` model along an arbitrary line defined using a list of x, y coordinate
 384 pairs (tuples) defining the vertices of the line. For structured grids, cross-sections can also be specified
 385 along a row or column.

```

386     >>> fx = flopy.plot.PlotCrossSection(model=gwf,

```

```

387 ... line={"line": [(0, 42500), (186801, 42500)]})
388 ...
389 >>> fx.plot_array(head, head=head)
390 >>> fx.plot_grid()
391 >>> plt.show()

```

The `head=` keyword option `plot_array()` method in the Python code demonstrated above limits the color flood to the saturated thickness of water in each cell. Figure 4C and D show the outcome of the Python code demonstrated along cross-section lines A–A' and B–B' (shown in Figure 4A) above with fine-grained control of grid lines, text, annotations, tick locations, and axis labels. Note that the color flood of head in Figure 4C and D shows that unconfined conditions occur in higher elevation cells or cells adjacent to river cells.

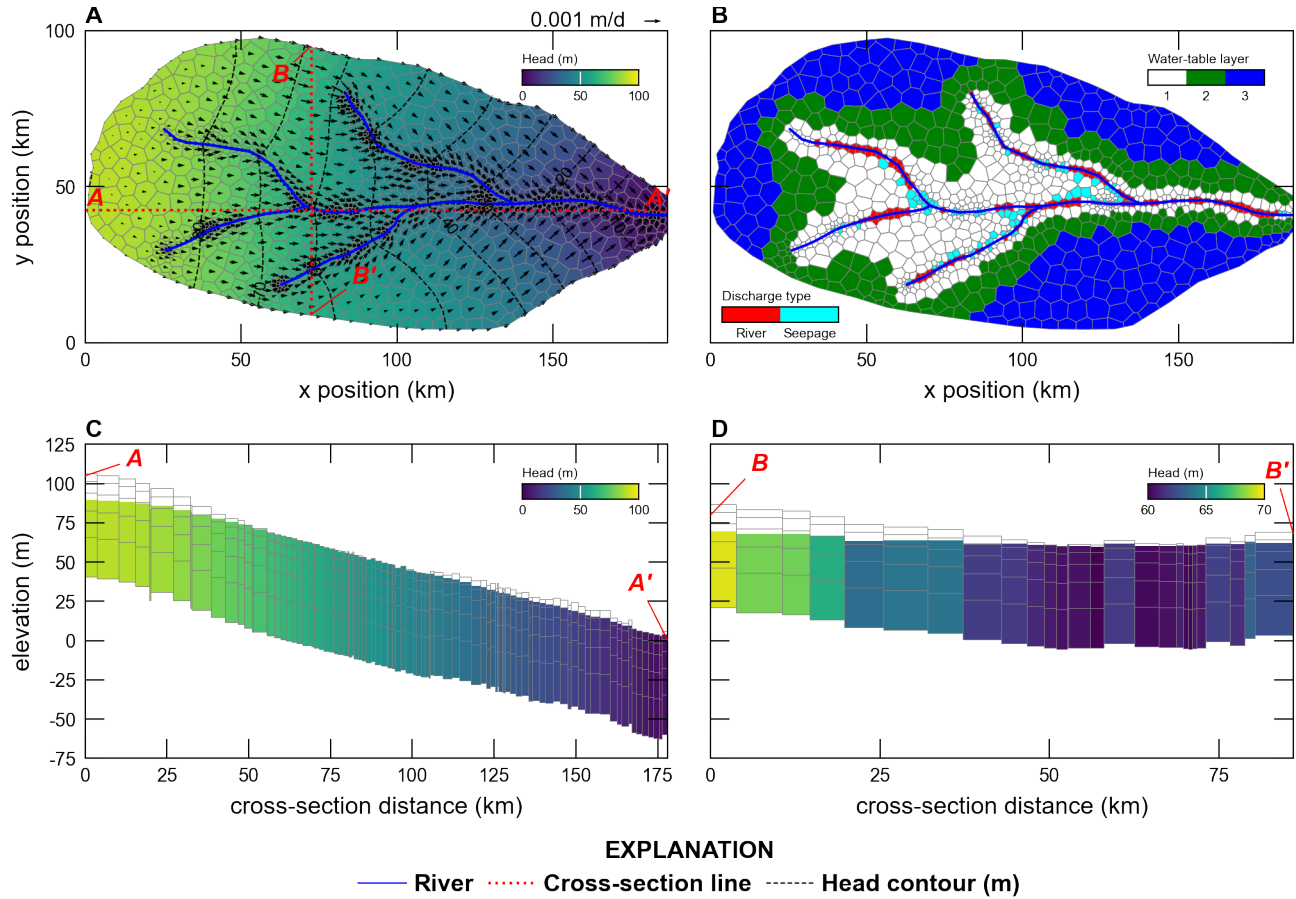


Figure 4: Examples of FloPy map and cross-section plotting capabilities for a model discretized using a Voronoi grid (Figure 2F). (A) Map showing simulated heads and specific-discharge vectors in the upper-most saturated cells. (B) Map showing the layer containing the water table, the location of cells where the aquifer is discharge to rivers represented as drain cells, and the location of cells where groundwater is discharging to the land surface. (C) East-West cross-section along line A–A', shown on Figure 4A, showing the model grid, simulated heads, and cells where water-table conditions exist. (D) North-South cross-section along line B–B', shown on Figure 4A, showing the model grid, simulated heads, and cells where water-table conditions exist.

398 **3.6 Exporting Grid Data to Other Formats**

399 Model input and output can be exported in a variety of standard formats using the `export()` method,
400 which is available for FloPy model objects, package objects, binary dependent-variable (head, con-
401 centration, *etc.*), and cell-by-cell output files. Standard output formats that are currently supported
402 include shapefiles ([ESRI 1998](#)), NetCDF files ([Rew et al. 2006](#); [Rew and Davis 1990](#)), and Visualiza-
403 tion Tool Kit (VTK) files ([Schroeder et al. 2006](#)). Entire models, packages, individual package arrays,
404 binary dependent-variables (for example heads), or three-dimensional representations of binary cell-by-
405 cell data can be exported. Shapefile and VTK output can be exported for all grid types but NetCDF
406 files can currently only be exported for structured grids. The NetCDF output capability has been used
407 to convert entire models and associated output so that it can be rendered in the GWWebFlow viewer
408 ([U.S. Geological Survey 2018](#)).

409 The following Python code demonstrates the steps for exporting the `gwf` model as a VTK dataset
410 with flat cell tops and bottoms (stair-case representation).

```
411 >>> gwf.export("temp_vtk/vtk_smooth", fmt='vtk', smooth=False,  
412 ... vertical_exaggeration=500.0, pvd=True)  
413 ...
```

414 VTK models can also be exported with smooth cell tops and bottoms using elevations interpolated to
415 the cell vertices. Other supported export formats can be created by specifying the file extension to be
416 `.shp` for shapefiles, `.nc` for NetCDF files, or if the `fmt` keyword is `vtk` (as shown above) for VTK files.
417 Figure 5 shows stair-case and smooth VTK exports of the model described in Section 3.5 and rendered
418 with Paraview ([Ahrens et al. 2005](#)).

419 **4 Scripting MODFLOW 6 Model Development Using Python and**
420 **FloPy**

421 In this section, FloPy is used to construct, run, and post process a MODFLOW 6 model. All pre-
422 and post-processing was done using FloPy grid, geospatial processing, MODFLOW 6 processing, and
423 plotting functionality discussed previously.

424 Hill et al. (1998) presented a synthetic test case (Synthetic Valley) of an undeveloped alluvial valley
425 surrounded by low permeability bedrock. The model included the Blue Lake and Straight River surface
426 water features (Figure 6A). The model presented in Hill et al. (1998) was simulated using MODFLOWP
427 ([Hill 1992](#)) using a structured grid with a constant 152.4 m grid spacing, three model layers, and 1,000
428 active cells per layer. The upper two layers represented an unconfined aquifer, and the third layer
429 represented a lower aquifer unit that is separated from the overlying aquifer by a confining unit in the
430 northern part of the model domain (Figure 6A). The confining unit was not explicitly represented in
431 Hill et al. (1998), instead a quasi-3D approach (low vertical conductance) between layers 2 and 3 was
432 used to represent the confining unit.

433 **4.1 MODFLOW 6 Model Setup**

434 To demonstrate that capabilities of FloPy and MODFLOW 6 the 6,096 m x 3,810 m model domain
435 is discretized using a Voronoi grid, with 6,343 active cells per layer, and the discretization by ver-
436 tices (DISV) package (Figure 6A). The model grid was developed using the `FloPy.Triangle()` and
437 `VoronoiGrid()` utility classes. The model grid was refined within Blue Lake, around Straight River
438 using a 750 m buffer length, and around pumping wells P1, P2, and P3 using a 100 m buffer length.

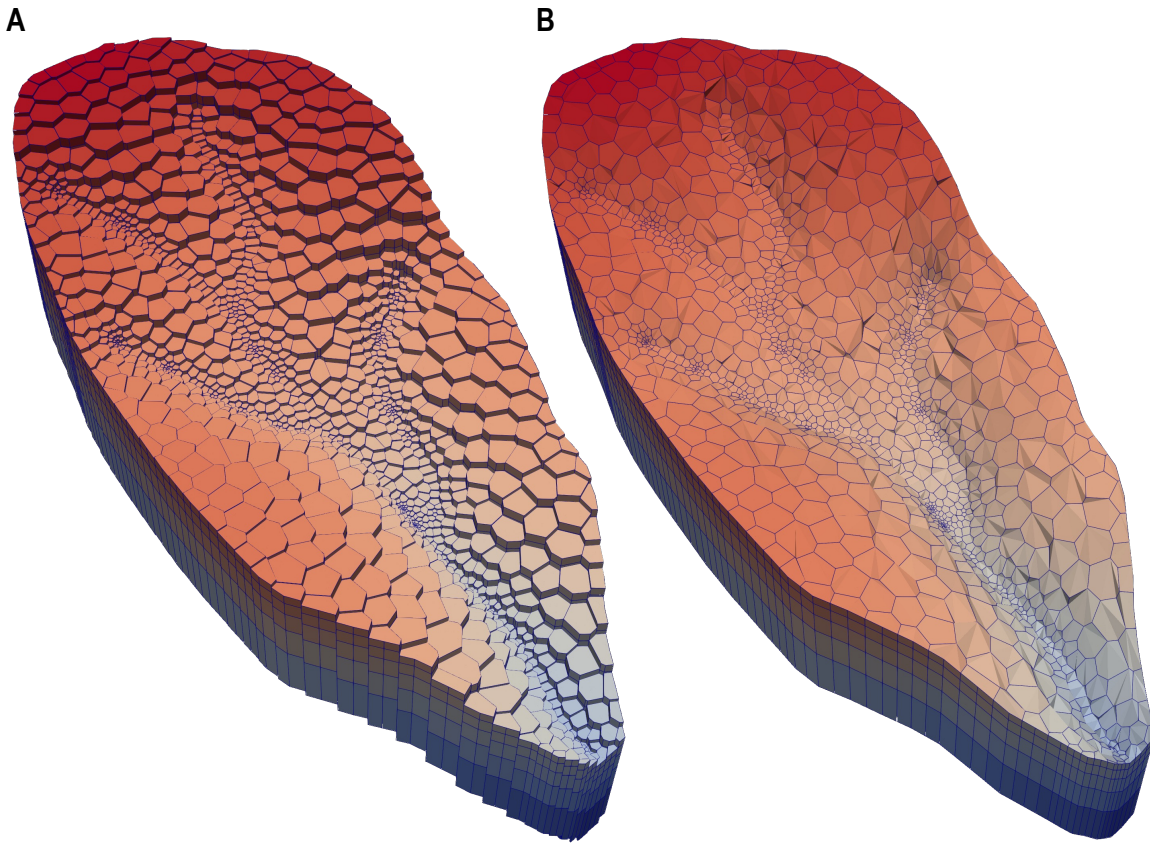


Figure 5: Two different graphical renderings of the Voronoi model grid: (A) stair-cased representation in which cell have flat tops and bottoms and (B) smooth representation in which elevations for cell vertices are interpolated using cell top and bottom elevations. Renderings were created using Paraview (Ahrens et al. 2005) and Visualization Tool Kit (Schroeder et al. 2006) files exported from FloPy.

In this example both groundwater flow and solute transport are simulated. As a result, the lower aquifer has been discretized into 3 layers (instead of one) to better represent solute transport. Confining units have to be explicitly simulated in MODFLOW 6, therefore, a total of six layers are simulated. The bottom of layers 1, 2, 3, and 4 were set to constant values of -1.53, -15.24, -15.55 and -30.48 m, respectively. In areas where the confining unit does not exist, the IDOMAIN concept (Langevin et al. 2017) was used to eliminate cells in model layer 3 (by setting IDOMAIN=-1) where the confining unit does not exist. In these areas, the bottom of layer 2 was set equal to the bottom of layer 3 (-15.55 m) and idomain was set to -1. The assignment of IDOMAIN equal to -1 marks these cells in layer 3 as “vertical pass through cells,” which means an overlying cell in layer 2 is directly connected to an underlying cell in layer 4.

The bottom of the model (layer 6) is based on Hill et al. (1998) and the bottom of layer 5 was specified to be half the distance between the bottom of layers 4 and 6. The top of the model was developed from topographic contours developed for model that was used as the starting point for Hill et al. (1998) (Pollock 2014); the top of the model is shown in Figure 7A. The top of the model and the bottom of layers 6 were resampled from the data used in the structured grid model using the `.resample_to_grid()` method and linear interpolation. Figure 9 shows the vertical discretization along cross-section lines A-A' and B-B', which are shown in Figure 7A. The groundwater flow and

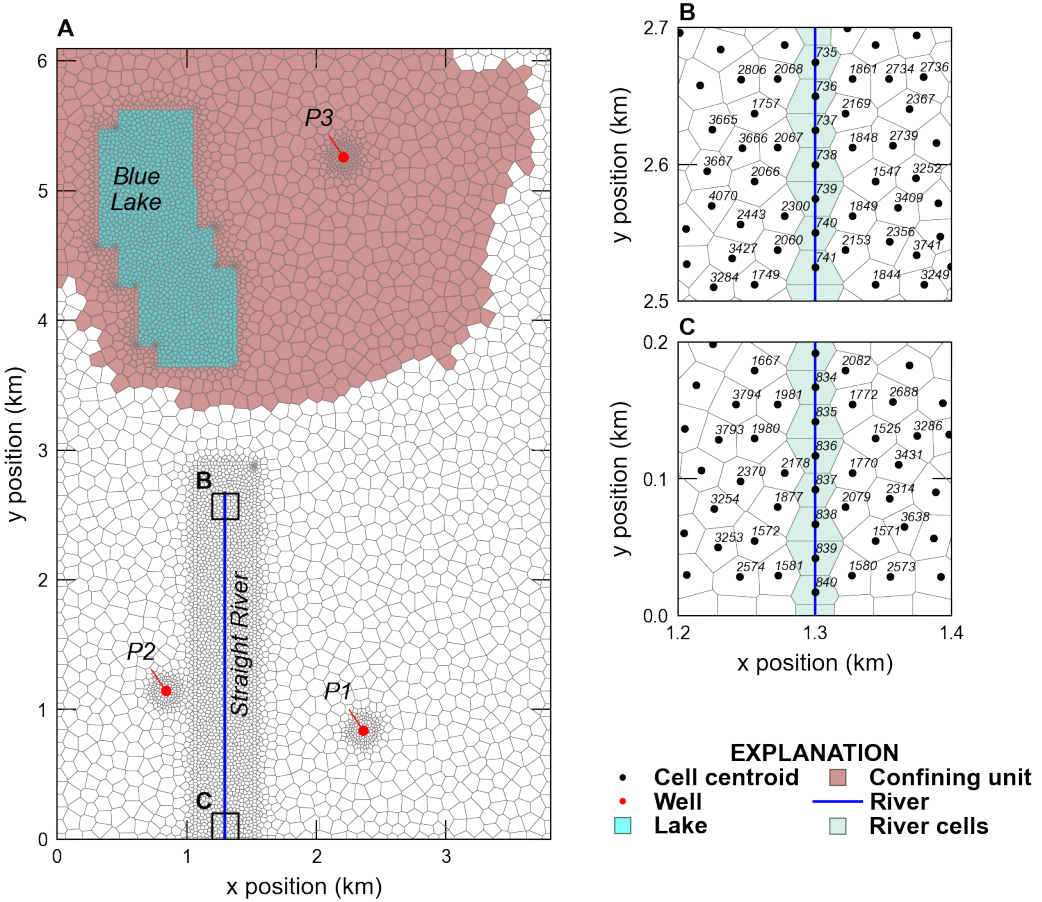


Figure 6: Synthetic Valley model used to demonstrate the MODFLOW 6 capabilities of FloPy. (A) Map showing the Voronoi grid used to discretized the model domain and the location of Blue Lake, Straight River, and the areal extent of the confining unit separating the upper and lower aquifer units. (B) Map showing model cells intersecting the northern end of Straight River. (C) Map showing model cells intersecting the southern end of Straight River. The cell centroid and cell numbers in the inset areas at the northern and southern end of Straight River are also shown on (B) and (C).

456 transport models were run for a total of 30 years. The groundwater flow model used a single steady-
 457 state time step and groundwater flow results were used to run the transport model with a total of 360
 458 time steps with a constant length of 30.4375 days.

459 Hydraulic properties for the model were resampled from the data used in the structured grid model
 460 that was used as the starting point for Hill et al. (1998) (Pollock 2014). The horizontal hydraulic con-
 461 ductivity was discretized into five zones with values of 45.72, 50.29, 60.96, 83.82, and 121.92 m/d; the
 462 lowest hydraulic conductivity zone was located south of Blue Lake and the highest hydraulic conduc-
 463 tivity zone was located beneath Blue Lake. The vertical hydraulic conductivity in the upper and lower
 464 aquifer was specified to be one quarter of the horizontal hydraulic conductivity. The horizontal and

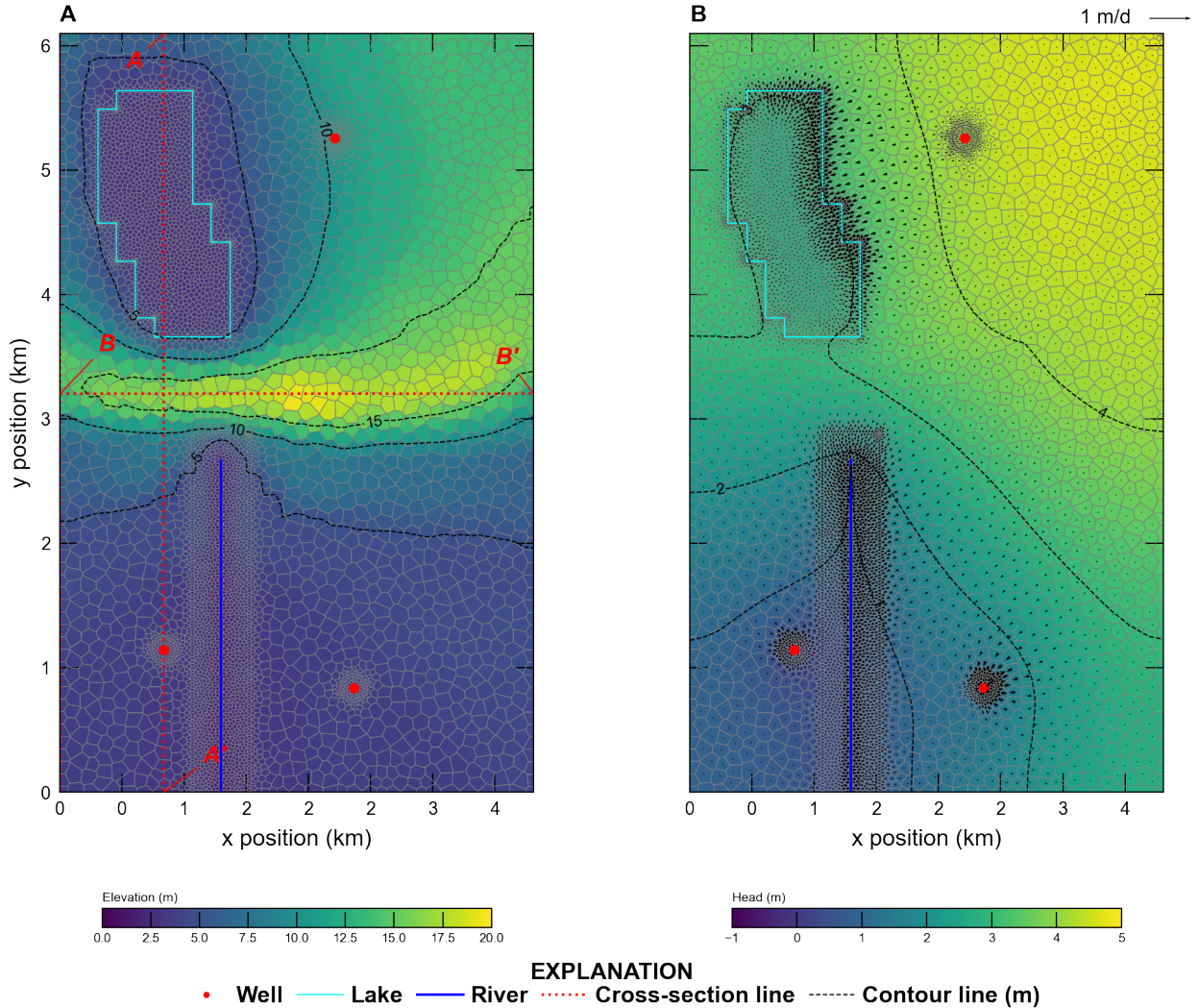


Figure 7: Map showing Synthetic Valley model (A) topography and (B) simulated steady-state heads and specific discharge rates in model layer 1. Cross-section lines A–A' and B–B' shown in Figure 9 are also shown on (A).

vertical hydraulic conductivity in the confining unit was set equal to 9.14×10^{-4} m/d. The horizontal and vertical hydraulic conductivity were resampled from the data used in the structured grid model using the `.resample_to_grid()` method and the nearest neighbor algorithm.

For the groundwater transport model the porosity was set to 0.2 in the upper and lower aquifer and 0.4 for cells in the confining unit. For the transport model, the Total Variation Diminishing scheme was used to simulate advection. Dispersion was simulated using a longitudinal dispersivity of 75 m and a transverse dispersivity of 7.5 m. Molecular diffusion was not represented.

In the Hill et al. (1998) representation of Synthetic Valley, the Straight River was simulated as head-dependent river (RIV) package cells, and Blue Lake was simulated as a high-hydraulic conductivity feature in model layer 1. In this FloPy recreation, Straight River is simulated using the streamflow routing (SFR) package, and Blue Lake is simulated using the LAK package. The location of the cells in model layer 1 with SFR or LAK package cells were determined using `GridIntersect().intersect()`

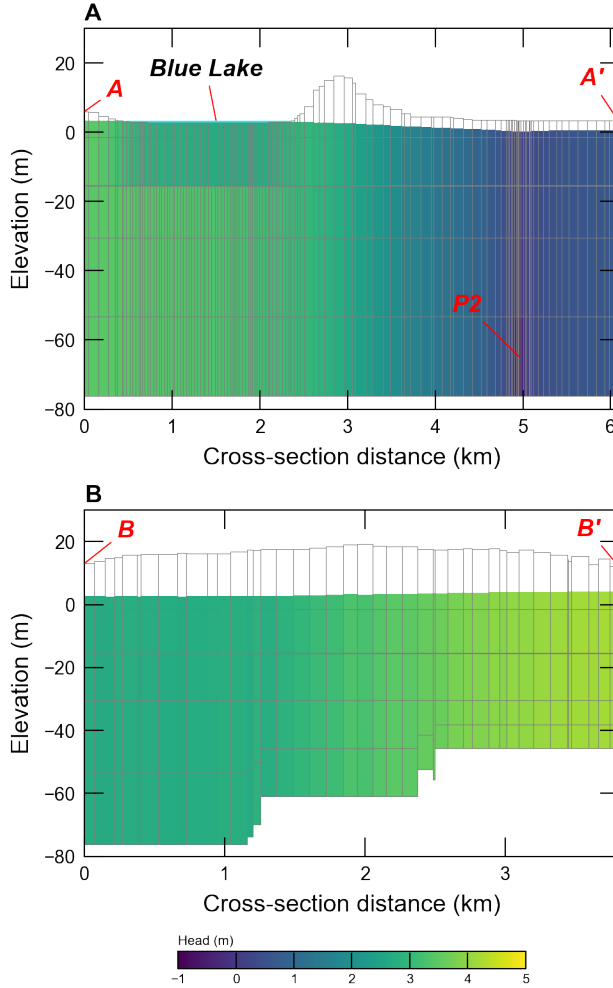


Figure 8: Cross-section of Synthetic Valley model grid and simulated steady-state heads along cross-section line (A) A–A' and (B) B–B'. The simulated Blue Lake steady-state stage (3.46 m) and pumping well P-2 are also shown on (A).

477 FloPy functionality (Figure 7A).

478 Straight River was discretized into 108 SFR reaches. Cells that intersect the northern and southern
479 end of Straight River are shown in Figures 7B and C. The bed thickness and width of each SFR reach
480 was specified to be 0.3048 and 3.048 m, respectively. The leakance for each SFR reach was calculated
481 using the bed thickness, reach width, and reach length in each cell and based on a total Straight River
482 conductance of 50,971.72 m²/d. A specified rainfall rate of 0.0025 m/d and a potential evaporation
483 rate of 0.0019 m/d was defined for each Straight River reach.

484 Blue Lake was simulated as a lake on top of the model grid and only had vertical connections to
485 1,406 cells in the underlying upper aquifer (model layer 1). A bed leakance of 0.0013 1/d was specified
486 for each cell connected to Blue Lake. A specified rainfall rate of 0.0025 m/d and a potential evaporation
487 rate of 0.0019 m/d was defined for Blue Lake.

488 Drain (DRN) cells were specified in each cell in model layer 1 that was not connected to Blue Lake
489 to prevent water levels from exceeding the top of the model. The conductance of each DRN cell was
490 based on the horizontal cell area, a thickness of 0.3048 m, and a vertical hydraulic conductivity of
491 0.03048 m/d. The drainage conductance was scaled from 0 to 100% of the specified conductance from

492 1 m below the top of the model to the top of the model, respectively.

493 Areal specified recharge and potential evapotranspiration rates of 0.0025 and 0.0019 m/d were
494 specified using the recharge (RCH) and evapotranspiration (EVT) packages, respectively. The EVT
495 surface was specified to be the top of the model and the EVT extinction depth was specified to be 1
496 m.

497 The location of pumping wells P1, P2, and P3 were determined using `GridIntersect().intersect()`
498 FloPy functionality (Figure 7A). Pumping rates of -7,600, -7,600, and -1,900 m³/d were specified for
499 pumping wells P1, P2, and P3, respectively.

500 Transport was not simulated in the LAK and SFR packages. Instead, a specified concentration
501 condition with a concentration of 1.0 mg/L was specified for Blue Lake. All other stress packages were
502 assumed to have a concentration of 0 mg/L.

503 An initial head of 11 m was specified for every cell. An initial stage of 3.44 m was specified for
504 Blue Lake. An initial concentration of 0 mg/L was specified for the transport model. 

505 4.2 Simulated Results

506 Simulated heads and vectors of specific discharge in model layer 1 are shown in Figure 7B. Specific
507 discharge is greatest on the east side of Blue Lake and in the vicinity of the three pumping wells and
508 Straight River. Cross-sections showing simulated heads along cross-sections A–A' and B–B' are shown
509 in Figure 9. The cross-sections show that water table conditions occur in most of the model domain
510 except in the vicinity of Blue Lake.

511 Simulated concentrations at the end of 30-years in all six model layers are shown in Figure 9.
512 Simulated concentrations are highest beneath Blue Lake in model layer 1 and do not vary much in
513 model layers 1 and 2. Simulated concentrations in model layer 3 are limited to the extent of the
514 confining unit because the remaining cells in the layer are defined to be vertical pass through cells
515 (`IDOMAIN=-1`). The lateral extent of the solute plume does not vary much south of Blue Lake because
516 of the lack of confinement in these areas.

517 5 Summary and Conclusions

518 FloPy is a [popular](#) Python package for building, running, and post processing groundwater models. It
519 is open source and developed with input from a growing community of contributors. This paper sum-
520marizes important new FloPy capabilities that have been added since the package was first described
521 by (Bakker et al. 2016). The new capabilities can be summarized as follows.

522 • FloPy supports the creation of many different types of groundwater models, including mod-
523 els that use MODFLOW 6, MODFLOW-2005, MODFLOW-NWT, MODFLOW-USG, MT3D,
524 MT3D-USGS, and SEAWAT. FloPy support for MODFLOW 6 is based on an entirely new ap-
525 proach designed to automatically support all MODFLOW 6 models, packages, and options. The
526 underlying FloPy classes for MODFLOW 6 are programmatically generated from the same input
527 definition files that are used to construct the MODFLOW 6 user guide. This correspondence
528 ensures that the FloPy classes are in direct correspondence with MODFLOW 6 input.

529 • FloPy has been extended to support unstructured model grids in addition to regular grids defined
530 by layers, rows, and columns. FloPy has several different routines for creating unstructured grids.
531 FloPy includes a wrapper for the GRIDGEN program (Lien et al. 2014), which can be used to
532 create layered quadtree grids. FloPy also includes a wrapper for the Triangle program (Shewchuk
533 1996), which can be used to create triangular meshes. A triangular mesh can be converted by
534 FloPy into a Voronoi grid. Grid information is stored for each FloPy model created by the user.

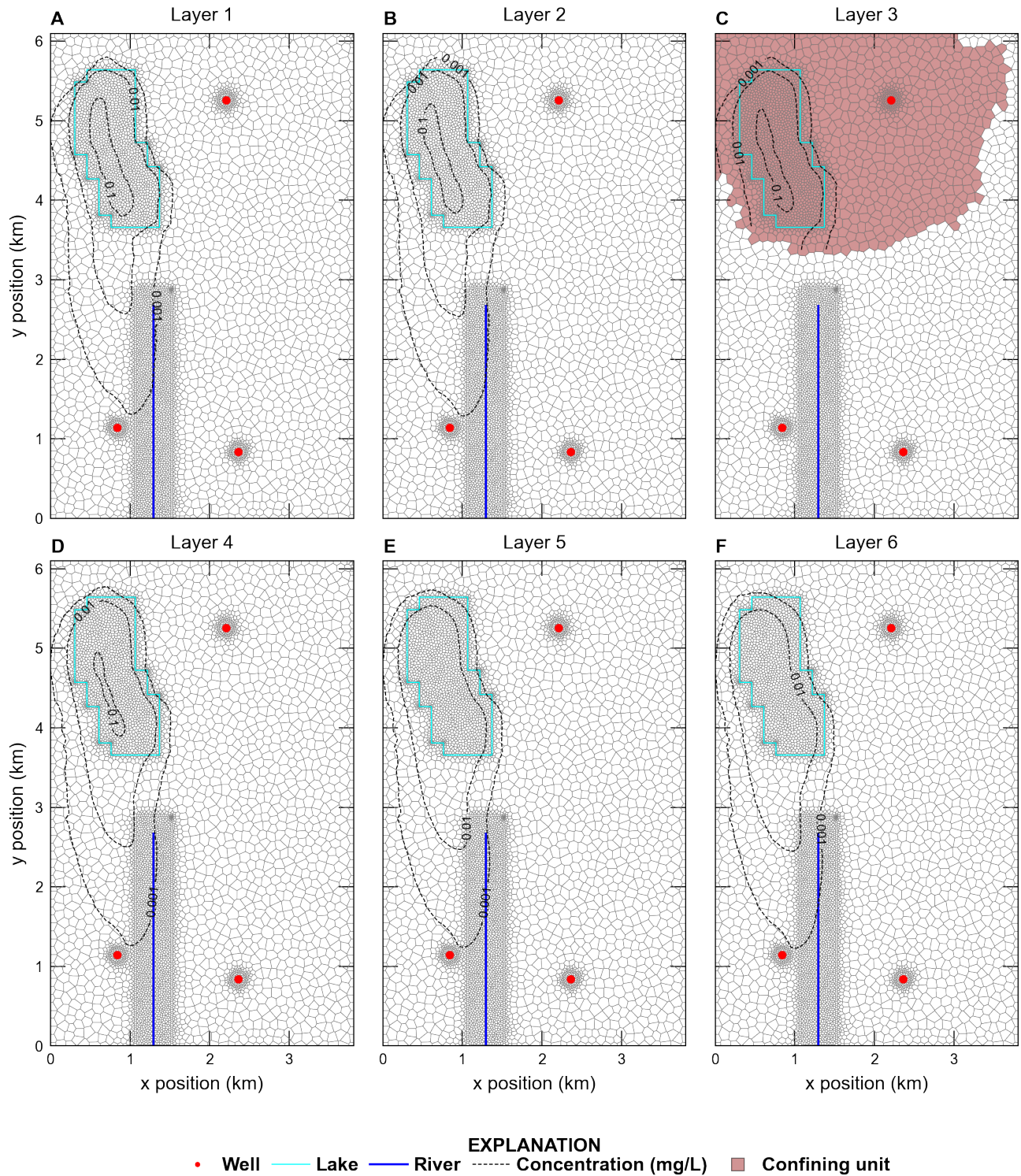


Figure 9: Maps showing Synthetic Valley simulated concentrations at the end of 30 years in model layer (A) 1, (B) 2, (C) 3, (D) 4, (E) 5, and (F) 6. The extent of the confining unit in model layer 3 is also shown on (C).

535 This model grid object is used systemically throughout FloPy for geospatial operations, plotting,
536 and exporting model information to supported formats.

- 537 • Geospatial intersections of points, lines, and polygons with model grids and raster resampling
538 onto model grids are common steps in model construction. FloPy fully supports these geospatial
539 operations through its grid intersection and raster resampling routines.
- 540 • Access to model output using FloPy has been simplified for MODFLOW 6 models. The new
541 output access routines makes it possible to quickly extract simulated results from binary and
542 text model output files.
- 543 • FloPy supports plan-view map and cross-section plotting of model grids, boundary conditions,
544 and simulated results. These plotting routines work with structured and unstructured models
545 and can be customized to produce high quality figures.
- 546 • FloPy supports the export of model information to shapefiles, VTK files, and NetCDF files. These
547 exported files can then be loaded into other software programs, such as geographic information
548 systems or advanced visualization programs for additional processing.

549 FloPy makes it possible to construct, and reproduce the construction, of a groundwater model
550 from native data in any format that can be accessed using Python. The robust new features in FloPy
551 allow users to quickly try different model grids, different model spatial and temporal resolution, and
552 different model configurations.

553 It is often useful to write a Python script to construct a groundwater model from start to finish.
554 The new geospatial processing routines make it possible to change model resolution as part of the
555 model construction script. This allows one to prototype fast running models with coarse resolution
556 and use finer resolution as the model starts to behave as intended. This workflow also allows one to
557 conduct grid convergence studies to ensure that the grid is not the cause of unintended model behavior.

558 Acknowledgments

559 The authors gratefully acknowledge the efforts of Mark Bakker and Vincent E.A. Post for initially
560 developing FloPy and their continued efforts improving FloPy. Funding for this research was provided
561 by the Enterprise Capacity (EC) project of the U.S. Geological Survey Integrated Water Prediction
562 program.

563 Data Availability Statement

564 FloPy is an open source software product and we welcome bug reports, code contributions, or im-
565 provements to the documentation from the community. The FloPy Python package can be installed
566 using `conda` or `pip`. The source code, code documentation, tutorials, and examples can be found in
567 the [FloPy GitHub repository](#). The Synthetic Valley example is available as a [MODFLOW 6 example](#)
568 and the hypothetical watershed grid examples are available on the [FloPy GitHub repository](#).

569 References

570 Ahrens, J., B. Geveci, and C. Law. 2005. ParaView: An End-User Tool for Large Data Visualization.
571 Visualization Handbook. Elsevier.

- 572 Bakker, M., V. Post, C.D. Langevin, J.D. Hughes, J. White, J. Starn, and M.N. Fienen. 2016. Scripting
573 MODFLOW model development using Python and FloPy. *Groundwater* 54, no. 5: 733–739, <https://doi.org/10.1111/gwat.12413>.
- 575 Befus, K.M., P.L. Barnard, D.J. Hoover, J.A. Finzi Hart, and C.I. Voss. 2020. Increasing threat of
576 coastal groundwater hazards from sea-level rise in California. *Nature Climate Change* 10, no. 10:
577 946–952, <https://doi.org/10.1038/s41558-020-0874-1>.
- 578 Befus, K.M., K.D. Kroeger, C.G. Smith, and P.W. Swarzenski. 2017. The Magnitude and Origin of
579 Groundwater Discharge to Eastern U.S. and Gulf of Mexico Coastal Waters. *Geophysical Research
580 Letters* 44, no. 20: 10,396–10,406, <https://doi.org/10.1002/2017GL075238>.
- 581 Burek, P., Y. Satoh, T. Kahil, T. Tang, P. Greve, M. Smilovic, L. Guillaumot, F. Zhao, and Y. Wada.
582 2020. Development of the Community Water Model (CWatM v1.04) – a high-resolution hydrological
583 model for global and regional assessment of integrated water resources management. *Geoscientific
584 Model Development* 13, no. 7: 3267–3298, <https://doi.org/10.5194/gmd-13-3267-2020>.
- 585 Ebeling, P., F. Handel, and M. Walther. 2019. Potential of mixed hydraulic barriers to remediate
586 seawater intrusion. *Science of The Total Environment* 693: 133478, <https://doi.org/10.1016/j.scitotenv.2019.07.284>.
- 588 ESRI. 1998. ESRI Shapefile Technical Description, an ESRI white paper. <http://www.esri.com/library/whitepapers/pdfs/shapefile.pdf> (accessed August 29, 2022).
- 590 Essawy, B.T., J.L. Goodall, W. Zell, D. Voce, M.M. Morsy, J. Sadler, Z. Yuan, and T. Malik. 2018.
591 Integrating scientific cyberinfrastructures to improve reproducibility in computational hydrology:
592 Example for HydroShare and GeoTrust. *Environmental Modelling & Software* 105: 217–229, <https://doi.org/10.1016/j.envsoft.2018.03.025>.
- 594 Fienen, M.N. and M. Bakker. 2016. HESS Opinions: Repeatable research: what hydrologists can learn
595 from the Duke cancer research scandal. *Hydrology and Earth System Sciences* 20, no. 9: 3739–3743,
596 <https://doi.org/10.5194/hess-20-3739-2016>.
- 597 Fienen, M.N., M.J. Haserodt, A.T. Leaf, and S.M. Westenbroek. 2022. Simulation of regional ground-
598 water flow and groundwater/lake interactions in the Central Sands, Wisconsin. Scientific Investigations Report
599 2022-5046, 111 p. <https://doi.org/10.3133/sir20225046>.
- 600 Gillies, S.. 2022. The shapely user manual. <https://shapely.readthedocs.io/en/stable/manual.html> (accessed August 28, 2022).
- 602 Gillies, S. et al.. 2013. Rasterio: geospatial raster I/O for Python programmers. <https://github.com/rasterio/rasterio> (accessed October 6, 2022).
- 604 Guira, M.. 2018. Numerical Modeling Of The Effects Of Land Use Change And Irrigation On Stream-
605 flow Depletion Of Frenchman Creek, Nebraska. Master's thesis, University of Nebraska, Lincoln,
606 NE.
- 607 Hill, M.C.. 1992. A computer program (MODFLOWP) for estimating parameters of a transient, three-
608 dimensional, ground-water flow model using nonlinear regression. U.S. Geological Survey Open-File
609 Report 91-484, 358 p.
- 610 Hill, M.C., R.L. Cooley, and D.W. Pollock. 1998. A Controlled Experiment in Ground Water Flow
611 Model Calibration. *Groundwater* 36, no. 3: 520–535, <https://doi.org/10.1111/j.1745-6584.1998.tb02824.x>.

- 613 Hughes, J.D., C.D. Langevin, and E.R. Banta. 2017. Documentation for the MODFLOW 6 framework.
614 U.S. Geological Survey Techniques and Methods, book 6, chap. A57, 36 p. <https://doi.org/10.3133/tm6A57>.
- 616 Hughes, J.D., S.A. Leake, D.L. Galloway, and J.W. White. 2022. Documentation for the Skeletal
617 Storage, Compaction, and Subsidence (CSUB) Package of MODFLOW 6. U.S. Geological Survey
618 Techniques and Methods, book 6, chap. A62, 57 p. <https://doi.org/10.3133/tm6A62>.
- 619 Hunter, J.D.. 2007. Matplotlib: A 2D graphics environment. *Computing in science & engineering* 9,
620 no. 03: 90–95.
- 621 Jaxa-Rozen, M., J.H. Kwakkel, and M. Bloemendal. 2019. A coupled simulation architecture for
622 agent-based/geohydrological modelling with NetLogo and MODFLOW. *Environmental Modelling
623 & Software* 115: 19–37, <https://doi.org/10.1016/j.envsoft.2019.01.020>.
- 624 Knowling, M.J., J.T. White, and C.R. Moore. 2019. Role of model parameterization in risk-based
625 decision support: An empirical exploration. *Advances in Water Resources* 128: 59–73, <https://doi.org/10.1016/j.advwatres.2019.04.010>.
- 627 Langevin, C.D., J.D. Hughes, A.M. Provost, E.R. Banta, R.G. Niswonger, and S. Panday. 2017. Doc-
628 umentation for the MODFLOW 6 Groundwater Flow (GWF) Model. U.S. Geological Survey Tech-
629 niques and Methods, book 6, chap. A55, 197 p. <https://doi.org/10.3133/tm6A55>.
- 630 Langevin, C.D., S. Panday, and A.M. Provost. 2020. Hydraulic-Head Formulation for Density-
631 Dependent Flow and Transport. *Groundwater* 58, no. 3: 349–362.
- 632 Langevin, C.D., A.M. Provost, S. Panday, and J.D. Hughes. 2022. Documentation for the MODFLOW
633 6 Groundwater Transport (GWT) Model. U.S. Geological Survey Techniques and Methods, book 6,
634 chap. A61, 56 p. <https://doi.org/10.3133/tm6A55>.
- 635 Leaf, A.T. and M.N. Fienen. 2022. Modflow-setup: Robust automation of groundwater model con-
636 struction. *Frontiers in Earth Science* 10: 903965, <https://doi.org/10.3389/feart.2022.903965>.
- 637 Lien, J.M., G. Liu, and C.D. Langevin. 2014. GRIDGEN Version 1.0: A computer program for
638 generating unstructured finite-volume grids. U.S. Geological Survey Open-File Report 2014–1109,
639 26 p. <https://doi.org/10.3133/ofr20141109>.
- 640 Mancewicz, L.K., A. Mayer, C.D. Langevin, and J. Gulley. 2022. Improved method for simulating
641 groundwater inundation using the MODFLOW 6 Lake Transport Package. *Groundwater*, <https://doi.org/10.1111/gwat.13254>.
- 643 Mehl, S.W. and M.C. Hill. 2006. MODFLOW-2005, the US Geological Survey modular ground-
644 water model-documentation of shared node local grid refinement (LGR) and the boundary flow and
645 head (BFH) package. U.S. Geological Survey Techniques and Methods, book 6, chap. A12, 78 p.
646 <https://doi.org/10.3133/tm6A12>.
- 647 Mehl, S.W. and M.C. Hill. 2013. MODFLOW-LGR—Documentation of ghost node local grid refine-
648 ment (LGR2) for multiple areas and the boundary flow and head (BFH2) package. U.S. Geological
649 Survey Techniques and Methods, book 6, chap. A44, 43 p. <https://doi.org/10.3133/tm6A44>.
- 650 Morway, E.D., C.D. Langevin, and J.D. Hughes. 2021. Use of the MODFLOW 6 water mover package
651 to represent natural and managed hydrologic connections. *Groundwater* 59, no. 6: 913–924, <https://doi.org/10.1111/gwat.13117>.

- 653 Panday, S., C.D. Langevin, R.G. Niswonger, M. Ibaraki, and J.D. Hughes. 2013. MODFLOW-USG
 654 version 1—An unstructured grid version of MODFLOW for simulating groundwater flow and tightly
 655 coupled processes using a control volume finite-difference formulation. U.S. Geological Survey Tech-
 656 niques and Methods, book 6, chap. A45, 66 p.
- 657 Pollock, D.W.. 2014. Personal communication. Reston, VA.
- 658 Provost, A.M., C.D. Langevin, and J.D. Hughes. 2017. Documentation for the “XT3D” Option in
 659 the Node Property Flow (NPF) Package of MODFLOW 6. U.S. Geological Survey Techniques and
 660 Methods, book 6, chap. A56, 46 p. <https://doi.org/10.3133/tm6A56>.
- 661 Rew, R. and G. Davis. 1990. NetCDF: an interface for scientific data access. *IEEE computer graphics*
 662 and applications
- 663 10, no. 4: 76–82.
- 664 Rew, R., E. Hartnett, J. Caron, et al.. 2006. NetCDF-4: Software implementing an enhanced data
 665 model for the geosciences. In *22nd International Conference on Interactive Information Processing*
Systems for Meteorology, Oceanograph, and Hydrology, Volume 6.
- 666 Rossetto, R., G. De Filippis, I. Borsi, L. Foglia, M. Cannata, R. Criollo, and E. Vázquez-Suñé. 2018.
 667 Integrating free and open source tools and distributed modelling codes in GIS environment for
 668 data-based groundwater management. *Environmental Modelling & Software* 107: 210–230, <https://doi.org/10.1016/j.envsoft.2018.06.007>.
- 669
- 670 Schroeder, W., K. Martin, and B. Lorensen. 2006. *The Visualization Toolkit* (4th ed.). Kitware.
- 671 Shewchuk, J.R.. 1996. Triangle: Engineering a 2D Quality Mesh Generator and Delaunay Trian-
 672 gulator. In *Applied Computational Geometry, Towards Geometric Engineering, FCRC'96 Work-
 673 shop, WACG'96, Philadelphia, PA, USA, May 27-28, 1996, Selected Papers*, pp. 203–222. <https://doi.org/10.1007/BFb0014497>.
- 674
- 675 Starn, J.J. and K. Belitz. 2018. Regionalization of Groundwater Residence Time Using Metamodeling.
 676 *Water Resources Research* 54, no. 9: 6357–6373, <https://doi.org/10.1029/2017WR021531>.
- 677 Sun, A.Y.. 2018. Discovering State-Parameter Mappings in Subsurface Models Using Generative Ad-
 678 versarial Networks. *Geophysical Research Letters* 45, no. 20: 11,137–11,146, <https://doi.org/10.1029/2018GL080404>.
- 679
- 680 U.S. Geological Survey. 2018. GWWebFlow—a browser-based groundwater model viewer. <https://webapps.usgs.gov/gwwebflow/>.
- 681
- 682 van Engelen, J., G.H. Oude Essink, H. Kooi, and M.F. Bierkens. 2018. On the origins of hypersaline
 683 groundwater in the Nile Delta aquifer. *Journal of Hydrology* 560: 301–317, <https://doi.org/10.1016/j.jhydrol.2018.03.029>.
- 684
- 685 Vilhelmsen, T.N., S. Christensen, and S.W. Mehl. 2012. Evaluation of MODFLOW-LGR in connection
 686 with a synthetic regional-scale model. *Groundwater* 50, no. 1: 118–132.
- 687 Virtanen, P., R. Gommers, T.E. Oliphant, M. Haberland, T. Reddy, D. Cournapeau, E. Burovski,
 688 P. Peterson, W. Weckesser, J. Bright, S.J. van der Walt, M. Brett, J. Wilson, K.J. Millman,
 689 N. Mayorov, A.R.J. Nelson, E. Jones, R. Kern, E. Larson, C.J. Carey, İ. Polat, Y. Feng, E.W.
 690 Moore, J. VanderPlas, D. Laxalde, J. Perktold, R. Cimrman, I. Henriksen, E.A. Quintero, C.R.
 691 Harris, A.M. Archibald, A.H. Ribeiro, F. Pedregosa, P. van Mulbregt, and SciPy 1.0 Contributors.
 692 2020. SciPy 1.0: Fundamental Algorithms for Scientific Computing in Python. *Nature Methods* 17:
 693 261–272, <https://doi.org/10.1038/s41592-019-0686-2>.

- 694 White, J.T.. 2018. A model-independent iterative ensemble smoother for efficient history-matching
695 and uncertainty quantification in very high dimensions. *Environmental Modelling & Software* 109:
696 191–201, <https://doi.org/10.1016/j.envsoft.2018.06.009>.
- 697 Zhou, Z. and D.M. Tartakovsky. 2021. Markov chain Monte Carlo with neural network surrogates:
698 application to contaminant source identification. *Stochastic Environmental Research and Risk As-*
699 *sessment* 35, no. 10: 639–651, <https://doi.org/10.1007/s00477-020-01888-9>.
- 700 Zipper, S.C., T. Gleeson, B. Kerr, J.K. Howard, M.M. Rohde, J. Carah, and J. Zimmerman. 2019.
701 Rapid and Accurate Estimates of Streamflow Depletion Caused by Groundwater Pumping Using
702 Analytical Depletion Functions. *Water Resources Research* 55, no. 7: 5807–5829, <https://doi.org/10.1029/2018WR024403>.